

Changing the physical and chemical properties of titanium oxynitrides $\text{TiN}_{1-x}\text{O}_x$ by changing the composition

Jesús Graciani,¹ Said Hamad,^{2,3} and Javier Fdez. Sanz^{1,*}

¹*Departamento de Química Física, Facultad de Química, Universidad de Sevilla, E-41012 Sevilla, Spain*

²*Instituto de Ciencia de Materiales de Sevilla, CSIC–Universidad de Sevilla, Avda. Américo Vespucio 49, 41092 Sevilla, Spain*

³*Department of Physical, Chemical and Natural Systems, University Pablo de Olavide, Carretera de Utrera, km 1, 41013 Sevilla, Spain*

(Received 7 June 2009; published 18 November 2009)

The stability and structural properties of titanium oxynitrides, $\text{TiN}_{1-x}\text{O}_x$, of different compositions are theoretically analyzed by means of first-principles periodic density-functional calculations. We show that at $x=0.55$ – 0.6 there is a change in the preferred structure from that of NaCl type to the α -TiO arrangement. For the NaCl-type structure the cell volume increases with x while it decreases with x for the α -TiO structure. The bulk moduli are always much larger for NaCl-type structures than for α -TiO and they decrease as the amount of O increases, moving from 280 GPa for TiN to 226 GPa for TiO (NaCl-type structure) or 197 GPa for α -TiO. Changes in the electronic structure with the composition are also considered. In general we found that in the two types of structure (NaCl and α -TiO), both the band gap and the ionic character increase with the O concentration.

DOI: [10.1103/PhysRevB.80.184112](https://doi.org/10.1103/PhysRevB.80.184112)

PACS number(s): 61.50.Ah, 71.15.Mb, 81.05.Je

I. INTRODUCTION

Titanium nitride is widely known as a refractory hard metal since it exhibits an extraordinary combination of properties:^{1,2} (i) ultrahardness (nearing that of diamond) and high melting point; (ii) brittleness, high thermal and electrical conductivities (higher than that of titanium metal), and even low-temperature superconductivity,^{3,4} and (iii) a NaCl-type ionic structure. Such an unusual combination of covalent, metallic, and ionic properties makes it a good candidate for technological applications in many areas as microelectronics,^{5–15} wear resistant coatings on cutting tools,^{16,17} dental surgery,¹⁸ decorative applications,¹⁹ and as potential sensors and catalysts.^{20,21}

On the other hand, titanium dioxide is a well-known semiconductor with many applications in some of the most important current research areas, such as solar energy harvesting,²² photocatalysis,^{23–27} and heterogeneous catalysis of supported metal nanoclusters.^{28–32} The easiness of preparation and stability of TiO_2 surfaces, in particular, the (110) face of rutile, make this material a real paradigm in surface science and catalysis.

A number of intermediate phases of general composition TiO_xN_y called “oxynitrides” are found midway between TiN and TiO_2 . Obviously the properties of the oxynitrides will be similar to those of the respective pure nitride and oxide when their compositions are close to those of the pure systems and are expected to change progressively from those of the nitride to those of the oxide and vice versa when the compositions move to intermediate values. However, concerning these materials a number of points are open: are those oxynitrides stable phases, i.e., able to synthesize? What are their structures? Are their properties a result of the combination of those of the pure solids? Are we really able to control these properties as a function of the composition TiO_xN_y ?

Preparation of oxynitrides through either oxidation of TiN or nitridation of TiO_2 constitutes a conspicuous problem. On one hand, the oxidation of the TiN quickly leads to formation

of TiO_2 .^{33,34} Only in some cases a very thin intermediate phase of mixed composition and unidentified structure has been observed between TiN and TiO_2 pure phases.^{35,36} Theoretical calculations have clearly shown that the oxidation of TiN under ordinary oxygen pressures leads to surface reconstructions of mixed composition and to the formation of amorphous TiO_2 on the reconstructed layer.^{18,34,37} Diffusion of O atoms to the bulk TiN has never been observed to occur in molecular-dynamics simulations, in fact the Ti atoms of the TiN surface actually move to the reconstructed layer to receive the incoming new oxygen molecules and form an incipient TiO_2 .³⁷ Similarly, N implantation on TiO_2 leads to large reconstructions of the surface due to a strong reduction and the reachable amount of implanted N is only 2–3%.³⁸ Previous density-functional theory (DFT) calculations³⁹ show that implanted N atoms need to be stabilized by an electronic transfer going from formally N^{2-} to the most stable configuration N^{3-} . Since the conduction band of TiO_2 is empty, the system needs to generate or to adsorb species with the ability to transfer electrons to the implanted N atoms (for example, oxygen vacancies, formally Ti^{3+} ions, or adsorbed metals).^{39–43}

No matter which preparation process we follow, oxidation of TiN or nitridation of TiO_2 , the resulting structure is metastable and not adequate to hold the optimal interactions between Ti and O atoms (or N atoms). However, while there is not any titanium nitride phase isostructural with TiO_2 , there is a stable Ti-O phase isostructural with TiN.^{44–48} This phase of TiO, namely, α -TiO, has a rock-salt structure in which an ordered substructure of both oxygen and titanium vacancies is superimposed on the original lattice. As a result the symmetry is shifted from cubic to monoclinic but the base rock-salt-type pattern remains. Thus, it should be much easier to synthesize an oxynitride of titanium from the nitridation of TiO since the incorporated N atoms are already in their most stable structure, namely, rock-salt structure. Moreover, in this way, the main drawback for the implantation of N in TiO_2 , the extra-electron transfer needed for closing the electronic

shell of the implanted N atoms in order to achieve their stabilization, is overcome since, in contrast with the semiconductor nature of TiO₂, α -TiO is a conductor and obviously the Ti 3d electrons of the conduction band are available for electronic transfers to the N atoms.

Therefore, taking α -TiO as starting point, one could expect that bulk phases of mixed compositions around TiN_{1-x}O_x with rock-salt structure might be obtained. Actually, it has been shown that this kind of oxynitride has new interesting properties, which can be controlled to be used in industrial applications. For example, the resistivity of TiO_xN_y thin films can be adjusted by regulating the x parameter, and the oxynitride's structural and chemical compatibility with TiN might be useful to build a new generation of nonvolatile memory devices.⁴⁹ Gradual transitions in conducting behavior, nanohardness, Young modulus, and color with the composition TiN_xO_y have been observed.^{19,50} As opposed to pure titanium nitride, titanium oxynitride nanocrystals with rock-salt structure and sizes of 15–35 nm have shown ultraviolet emission at room temperature in photoluminescence spectra.⁵¹ Finally, Ti-O/Ti-N systems are regarded as promising biocompatible materials, with possible applications in artificial heart valves.^{52,53}

In this work we study, by means of periodic DFT calculations, the stability of the phases TiN_{1-x}O_x in the range of compositions $x=0-1$, as well as, how the electronic, structural, and physical properties change with the composition. To this end, once the model has been defined, we studied exhaustively all the possible configurations for each composition and each structure (namely, NaCl type, cubic, or α type, monoclinic), which gives us additional confidence on the validity of our results. This exhaustive and systematic study of all the configurations has been possible thanks to the use of the SOD (site-occupancy disorder) code.⁵⁴ Finally, we analyze the energies and geometries involved in the first steps of the N-implantation process of α -TiO.

II. MODELS AND COMPUTATIONAL DETAILS

DFT calculations were performed using the plane-wave-pseudopotential approach within the projector-augmented wave method⁵⁵ together with the generalized gradient approximation exchange-correlation functional proposed by Perdew *et al.*,⁵⁶ as implemented in the VASP 4.6 code.^{57,58} A plane-wave cutoff energy of 500 eV was used. We treated the Ti(3s, 3p, 3d, 4s), O(2s, 2p), and N(2s, 2p) electrons as valence states while the remaining electrons were kept frozen as core states. The Brillouin-zone integrations were performed using Monkhorst-Pack grids.⁵⁹ We chose a supercell model of (1×1×3) for TiN (24 atoms) and one of (1×1×1) for α -TiO (20 atoms). These models allow us to change the composition progressively while still having a computationally affordable size since we optimize the geometries with high accuracy (cutoff of 500 eV, saturation of k points and demanding convergence criterions) for all the possible different independent configurations for each composition (240 calculations in total). The calculations were carried out using a (7×7×3) mesh for TiN and oxynitrides with NaCl-type structure, and a (6×4×6) mesh for TiO and ox-

ynitrides with α -TiO-type structure. The number of k points was selected in order to get TS corrections to the energy smaller than 0.001 eV/atom, as well as negligible changes in the optimized cell parameters. To obtain faster convergence with respect to the number of k points, thermal smearing of one-electron states ($k_B T=0.05$ eV) has been allowed using the Methfessel-Paxton scheme of order 1 to define the partial occupancies.

Forces on the ions were calculated using the Hellmann-Feynman theorem, as the partial derivatives of free energy with respect to the atomic position, including the Harris-Foulkes⁶⁰ correction to forces. This calculation of the forces allows the calculation of geometry optimizations using the conjugate-gradient scheme. Each self-consistent loop was stopped when the total free-energy change and the band-structure energy change (change in eigenvalues) between two steps were both smaller than 10^{-6} eV. Iterative relaxation of atomic positions was stopped when all forces were smaller than 10^{-2} eV/Å. With these criteria, forces on the atoms generally were less than 5×10^{-3} eV/Å.

As we mentioned above, we have performed an exhaustive study of all the possible configurations of the systems, i.e., we studied all the different arrangements of the N and O atoms in the unit cells. For example, if we want to model a TiN_{1-x}O_x system with NaCl-type structure, in which the N/O ratio is 0.5, we use the supercell (1×1×3) for TiN (which has 24 atoms), and we substitute six out of the 12 N atoms by O atoms. The number of different possibilities in which we can carry out the six substitutions is 940. In principle, if we wanted to make sure that we have found the most stable configuration of the system TiN_{0.5}O_{0.5} we should perform the 940 geometry optimizations, which would be an impossible task, given the current computer time limitations. In order to perform the exhaustive study of all the configurations while still using an acceptable amount of computer resources, we employed the SOD code,⁵⁴ which makes use of the symmetry of the system to reduce drastically the number of configurations.

In the previous example, most of the 940 configurations are found to be equivalent. Two configurations are equivalent when they are related by an isometric operation (such as translations, rotations, or reflections within the supercell, which are consistent with the symmetry operations of the crystal). Using the SOD code to remove the equivalent configurations we find that the number of nonequivalent configurations of the cited example is only 34, which is tractable with our computer resources. Employing the SOD code we also performed a statistical analysis of all the possible configurations of the TiN_{0.5}O_{0.5} system, with which we obtained the energy of the system as a weighted average of the 940 configurations. This average is calculated as follows. The system of N possible configurations (in the previous example $N=940$) is assumed to be at equilibrium at temperature T . Each configuration n (with energy E_n) in the complete space of configurations ($n=1, \dots, N$) can be assigned an occurrence probability,

$$P_n = \frac{1}{Z} \exp(-E_n/kT),$$

where $k=8.6173 \times 10^{-5}$ eV/K is Boltzmann's constant and

TABLE I. Formation energy, cell parameters, bulk moduli, and density for the most stable mononitride and monoxide of Ti, namely, TiN and α -TiO.

	TiN		α -TiO	
	Theory	Expt.	Theory	Expt.
Formation energy (kJ/mol)	-342.6	-337.7 ^a	-505.3	-519.7 ^d
a (Å)	4.254	4.238 ^b	5.856	5.855 ^e
b (Å)			9.344	9.340 ^e
				4.142 ^e
c (Å)			4.170	4.176 ^f
				4.170–4.190 ^g
γ			107° 38'	107° 32' ^e
Bulk modulus (GPa)	280	288 ^c	197	199–210 ^h
Density (g/cm ³)	5.34	5.21 ^d	4.87	4.95 ^d
				4.87–5.06 ^g

^aReference 68.^bReference 63.^cReference 64.^dReference 67.^eReference 45.^fReference 66 (at 100 K).^gReference 47 (at 300K).^hReference 65.

$$Z = \sum_{n=1}^N \exp(-E_n/kT)$$

is the partition function. The energy of the system is therefore

$$E = \sum_{n=1}^N P_n E_n.$$

If there is a big difference in energy between the most stable and the rest of the configurations, the Boltzmann's factor associated to that configuration will be much larger than the rest, and it will be the only configuration contributing to the average energy of the system. If there is no such big difference in energy between the most stable configuration and the rest, it is a better approximation to use the average energy explained above, than using only the energy of the most stable configuration. The SOD code has been successfully used in a range of different systems.^{54,61,62}

In order to study the $\text{TiN}_{1-x}\text{O}_x$ systems with NaCl-type structures, for $x=0, 0.16, 0.33, 0.5, 0.66, 0.83,$ and 1 , we substituted respectively $0, 2, 4, 6, 8, 10,$ and 12 of the 12 N atoms in the NaCl-type TiN supercell by O atoms. Using the SOD code we calculated the number of nonequivalent configurations, which is $1, 5, 21, 34, 21, 5,$ and 1 , respectively. The total number of configurations we studied with the NaCl-type structure is therefore 88 .

In the case of the $\text{TiN}_{1-x}\text{O}_x$ systems with α -TiO structures, the supercell had ten Ti atoms and ten N or O atoms. The concentrations studied are $x=0, 0.2, 0.4, 0.6, 0.8,$ and 1 , which are achieved by substituting $0, 2, 4, 6, 8,$ and 10 of the ten O atoms in the α -TiO supercell by N atoms. The number

of nonequivalent configurations in this case is $1, 15, 60, 60, 15,$ and 1 , respectively, giving a total number of 152 . Note that, even with a smaller number of atoms in the supercell (20 as opposed to 24), the number of nonequivalent configurations in the case of the α -TiO structure is almost twice as large as that in the case of the NaCl-type structure. The reason of that is the high symmetry of the latter structure, which allows a great reduction in the number of configurations.

III. RESULTS AND DISCUSSION

In order to test the accuracy of the methods used to study these systems, we show first the energetic and structural data of the pure solids: TiN and α -TiO. As shown in Table I, the formation energy, the optimized cell parameters, the bulk moduli, and the density are in good agreement with the experimental data.^{63–68}

The first and most crucial question we have to answer in this work is whether it is thermodynamically possible to synthesize oxynitrides. In other words, we have to study whether oxynitrides are stable with respect to the segregation in two oxide/nitride phases. It is worth noting that we have studied all the possible configurations N/O for each x value of the systems $\text{TiN}_{1-x}\text{O}_x$ in our supercell models. We have found that there is no thermodynamic driving force favoring segregation. In fact, the segregated configurations are among the most unstable for each x composition. This result opens the door to the synthesis of real oxynitrides. If until now they have not been synthesized successfully it might be due to an unsuccessful synthesis route, not to thermodynamic obstacles. TiN has tendency to generate quickly TiO_2 in presence of O_2 and TiO_2 has not tendency to admit implanted N

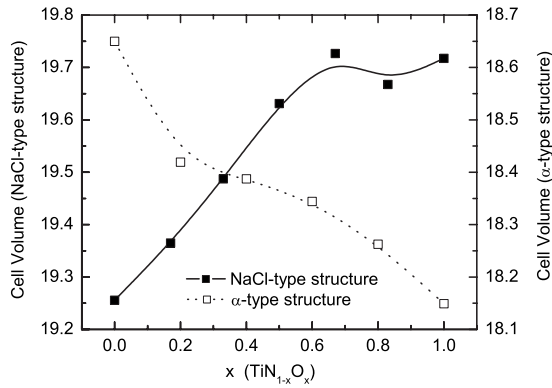


FIG. 1. Evolution of the cell volume of the oxynitrides per Ti atom ($\text{\AA}^3/\text{Ti}$ atom) with the composition ($x:\text{TiN}_{1-x}\text{O}_x$) for both structures NaCl type (black squares) and α type (white squares).

due to electronic reasons. But, as we mentioned in Sec. I, $\alpha\text{-TiO}$ could be an excellent candidate as initial compound to synthesize NaCl-type $\text{TiN}_{1-x}\text{O}_x$ compounds. We start our study with the structural characterization of these compounds.

A. Structural characterization

The cell parameters of the NaCl- and α -type structures of $\text{TiN}_{1-x}\text{O}_x$ evolve differently with x (see Fig. 1). In the former case the cell parameter increases with x while in the later case decreases. This result is in agreement with the experimental observations, in which the cell parameter of TiO increases as the amount of nitrogen implanted in the structure increases.⁶⁹ This behavior may be explained using the theoretical background established in a previous work.⁴⁸ The vacancies of both Ti and O atoms stabilize the α structure of TiO by a strong repolarization of the d band. This charge redistribution generates strong metal-metal bonds through and around oxygen vacancies and recovers a great part of the Madelung energy lost by the presence of the vacancies. The recovery of the Madelung energy is due to the accumulation of charge in the oxygen vacancies and the depletion of electron density in the titanium vacancies which, at the same time, decreases the electrostatic repulsion between the cations around the oxygen vacancies and between the anions around the titanium vacancies. Any loss of electron density in the $3d$ band of this solid will result in a loss of stability since the vacancy-mediated stabilization mechanism is based on this electron density. When oxygen atoms are replaced by nitrogen, formally one $3d$ electron of the system is lost since N atoms need three electrons to close its shell (N^{3-}) while the O atoms only need two (O^{2-}). So, the $3d$ population, which is responsible for the higher relative stability of the α structure with respect to the NaCl-type one, decreases as the amount of implanted N increases. This decrease in $3d$ population results in a weakening of metal-metal bonding through and around the oxygen vacancies, and it also induces an increase in the electrostatic repulsion between the cations around the oxygen vacancies. The presence of N^{3-} species instead of O^{2-} increases also the electrostatic repulsion between the anions around the titanium vacancies. The de-

crease in the strength of Ti-Ti bonds and the increase in electrostatic repulsions involve obviously an expansion of the crystal lattice. All these consequences of the presence of additional N atoms explain why the cell parameter of $\alpha\text{-TiN}_{1-x}\text{O}_x$ increases with the amount of N (i.e., why it decreases as x increases). Furthermore, basic considerations about the radii of the ions N^{3-} and O^{2-} may help us to understand this expanding behavior. However, these criteria based on atomic radii are not enough to explain completely the results, as one can deduce from the case of NaCl-type structure $\text{TiN}_{1-x}\text{O}_x$ compounds, which we are going to show in what follows.

In the case of the NaCl-type structure, the cell parameter increases with the amount of O, which has a smaller anion radius than N. One could consider that the filling of the d band when replacing N by O may be involved in the explanation of this behavior. However, the expected behavior would be just the opposite. For example, in the case of the consecutive NaCl-type nitrides of the early transition metals Sc, Ti, and V, the d band fills up progressively moving from ScN to VN while the factor of the Madelung potential is formally the same (NaCl structure and $\text{M}^{3+}\text{-N}^{3-}$ ions). The cell parameter decreases as the d band fills up 4.539 \AA (4.440 \AA) for ScN, 4.254 \AA (4.238 \AA) for TiN, and 4.129 \AA (4.137 \AA) for VN (experimental values in parenthesis).⁷⁰ The d bands of these solids come mainly from the metal-metal bonds. Therefore, the filling of the d band induce an increase in the metal-metal bond and the subsequent decrease in the cell parameter.

Then, neither the size of the anions nor the filling of the $3d$ band can explain the increase in the cell parameter of NaCl-type $\text{TiN}_{1-x}\text{O}_x$ compounds with x . The explanation may come from simple Madelung-potential considerations. When we move from TiN to TiO (both in their ideal NaCl-type structure) the formal charge of the periodically ordered ions change from $\text{Ti}^{3+}\text{-N}^{3-}$ to $\text{Ti}^{2+}\text{-O}^{2-}$, and consequently the electrostatic attractions change from a factor 9 to a factor 4. In fact, the lattice energies obtained from the application of the Born-Fajans-Haber cycle are 8033 and 3811 kJ/mol for TiN and TiO , respectively.⁶⁷ This may explain why the cubic TiO is less dense than TiN, despite the O^{2-} anions being smaller than N^{3-} and having the d band of TiO more electron population than the d band of TiN.

B. Simulation of the structural evolution of the $\text{TiN}_{1-x}\text{O}_x$ system with the composition

The structural evolution of $\text{TiN}_{1-x}\text{O}_x$ compounds has been studied through the evolution of the formation energy with both the composition (x) and the structure (NaCl and α). The formation energy was calculated as follows:

$$E_f(\text{TiN}_{1-x}\text{O}_x) = E(\text{TiN}_{1-x}\text{O}_x) - nE(\text{Ti bulk}) - \frac{n(1-x)}{2}E(\text{N}_2) - \frac{nx}{2}E(\text{O}_2),$$

where n is the number of Ti atoms, $E(\text{Ti bulk})$ is the energy of the bulk of metallic Ti per Ti atom, and $E(\text{N}_2)$ and

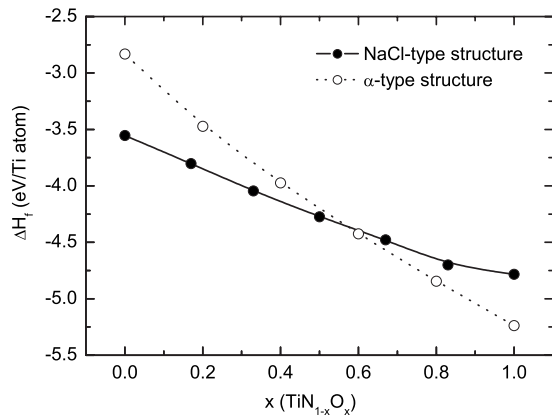


FIG. 2. Evolution of the formation energy of the oxynitrides per Ti atom (eV) with the composition (x : $\text{TiN}_{1-x}\text{O}_x$) for both structures NaCl type (black circles) and α type (white circles).

$E(\text{O}_2)$ are the energies of the isolated N_2 and O_2 molecules, respectively. $E(\text{TiN}_{1-x}\text{O}_x)$ is the free energy of the system obtained with the SOD code, which is calculated as the Boltzmann average of the free energies (calculated as the energy of the system minus the entropic term, TS_{conf} , where S_{conf} is the configurational entropy) of all the independent configurations for each particular value of x .

Obviously, when x is close to 0 the system will have tendency to arrange itself as NaCl-type structure since that is the most stable structure for TiN. Analogously, when x is close to 1 the system will try to arrange itself as α structure since this is the most stable structure for TiO. What we have to calculate is the limiting composition at which the change in crystal structure takes place, and whether this limiting composition depends on the temperature. Figure 2 shows the evolution of the formation energy with the composition for both structures at 10 K. It is worth noting that the entropic terms associated with the configurational entropies are very low (typically on the order of 0.1 meV/K), and they are also very similar for all configurations since there is no configuration with a number of equivalent configurations significantly higher than the rest (which could have much larger configurational entropy). As a result, entropy does not play a crucial role in our systems, i.e., in the temperature range between 10 and 600 K the entropic terms are much smaller than the difference in energy between the different configurations.

As expected, the NaCl-type structure is the preferred one for compositions close to $x=0$ (TiN) while the α structure is the most stable for compositions close to $x=1$ (TiO). The crossing point is found to be at the limiting composition of $x=0.55-0.60$, approaching 0.60 as the temperature increases (the curves were calculated at 10, 300, and 600 K but the difference between the curves at the three temperatures are very small, ≈ 0.01 eV/Ti atom). The system will tend to acquire the NaCl-type structure for compositions $x < 0.6$ while it will tend to be ordered as α structure for compositions $x > 0.6$. In the latter case one should expect to find a number of vacancies in both Ti and N/O sublattices since this is one of the main characteristics of the α structure. This is important from a technical point of view since the presence

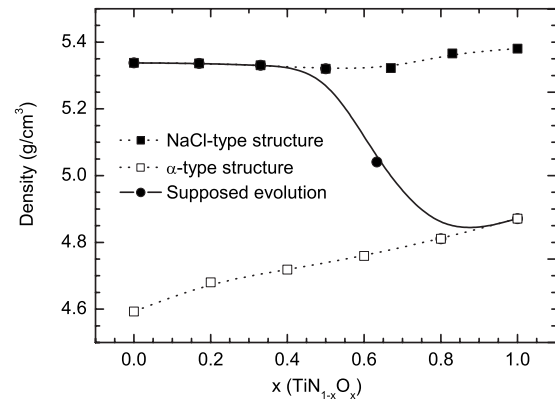


FIG. 3. Evolution of the density of the oxynitrides with the composition (x : $\text{TiN}_{1-x}\text{O}_x$) for both structures NaCl type (black squares) and α type (white squares), and the supposed evolution of the density taking into account the change in structure around $x=0.6$ (solid line and black circles).

of vacancies may drastically change the surface stability of the solid and generate highly reactive surfaces, which would be a serious drawback for microelectronic devices or technologies based on thin films but it could become interesting from a chemical point of view.

Initially, one could think that the limiting composition at which the system changes its structure should be placed at $x=0.5$ since at that composition the amount of N atoms (which tend to move the structure of the system to NaCl type) and the amount of O atoms (which tend to shift the structure of the system to the α type) is equal. However the limiting composition is shifted to higher values of x . This is due to the critical dependence of the stability of α structure on the $3d$ population.⁴⁸ This ordered defective structure is more stable than the regular NaCl type if, and only if, the system has enough $3d$ electrons to achieve the vacancy-mediated stabilization mechanism.⁴⁸ Since the incoming N atoms are emptying the $3d$ band, such stabilization mechanism is soon weakened and the NaCl-type structure becomes more stable than the α structure before the equal composition $x=0.5$ is reached.

C. Evolution of the physical properties

As the cell parameter is quite similar in both cases and it changes continuously with the composition, it could be difficult to determine experimentally if a nitrated/oxidized system of general composition $\text{TiN}_{1-x}\text{O}_x$ has NaCl-type or α structure, based only on the cell-parameter determination. For that reason, it would be useful to have another experimental observable for which the difference between them is more significant. This observable could be the density since the high concentration of vacancies in the α structure induces a significant decrease in the density of the solid with respect to the highly compact NaCl-type structure. In Fig. 3 we show the expected evolution of the density with the composition. For compositions below the limit ($x=0.6$) we have supposed NaCl-type structure and we have calculated the density using the average volume resulting from all the possible configurations, taking into account the statistic weight of each con-

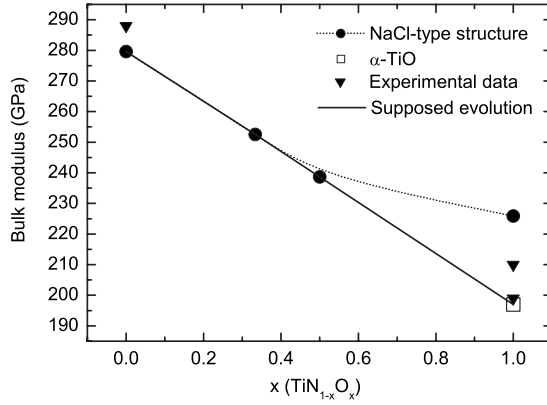


FIG. 4. Evolution of the bulk modulus of the oxynitrides with the composition (x : $\text{TiN}_{1-x}\text{O}_x$) for the NaCl-type structure.

figuration. The same procedure has been followed with the configurations of the α structure, for compositions $x > 0.6$. For the limiting composition ($x=0.6$) we have calculated the density supposing a system in which both structures are present in the same amount since both have the same formation energy. As can be seen in Fig. 3, the changes in density are large enough to be easily detected by experimental methods. This will be useful for experimental characterization purposes since density is an observable easily measurable, which changes significantly when the predominant structure changes.

However, one of the most interesting physical properties of these solids is their good mechanical behavior. For that reason, we have calculated the bulk moduli of the most stable configurations for different compositions. The results are shown in Fig. 4. The evolution of the bulk moduli of NaCl-type structure $\text{TiN}_{1-x}\text{O}_x$ with the composition shows a clear decreasing behavior with x . The higher the amount of O the lower the bulk moduli, being the calculated limit values of bulk moduli 280 GPa for $x=0$ (TiN) and 197 or 226 GPa for $x=1$ for α -TiO or NaCl-type structure TiO, respectively, (which is in good agreement with the experimental values: 288 and 199–210 GPa, respectively).^{64,65} We have also performed calculations for the α structure for small amounts of implanted N, in which we have found the same tendency, in general, the bulk moduli increases with the amount of N. In Fig. 4 we can see that the decreasing evolution of the bulk moduli with x is more pronounced for larger concentrations of N, and it becomes softer for high O concentrations. The same behavior has been observed in the α structure; the increasing evolution of the bulk moduli for small concentrations of N in α -TiO is much less pronounced than the decreasing evolution for NaCl structure for small concentrations of O. On the other hand, it is worth noting that bulk moduli of NaCl-type structures are much higher than those of α structures. Therefore, we can draw two conclusions: (a) bulk moduli increase as the amount of N increases and decrease as the amount of O increases; (b) for high N/O ratios the changes in the mechanical properties with the composition are higher than for low N/O ratios. So, in principle, we could modulate the mechanical properties of oxynitrides of titanium by controlling the composition $\text{TiN}_{1-x}\text{O}_x$, knowing that much higher bulk moduli will be

reached with the NaCl-type structure, i.e., with compositions $\text{TiN}_{1-x}\text{O}_x$ ($x < 0.6$).

D. First steps of the nitridation of α -TiO

As we mentioned in Sec. I, oxidation of TiN is a bad choice if one tries to synthesize oxynitrides of titanium with NaCl-type structure since the system quickly evolves to TiO_2 . However, α -TiO is a very good candidate as a starting compound for the synthesis of those oxynitrides. We have carried out calculations of the first steps of the nitridation process of α -TiO. In order to model adequately the initial isolated N-implanted species we have used a larger supercell of $(1 \times 1 \times 2)$ (40 atoms), reducing the k -points mesh to $(6 \times 4 \times 4)$. Initially there are two possibilities: substitutional (replacing one O) and in vacancies. In the latter case one could consider implantation of N in both types of vacancies, namely, Ti and O vacancies. Implantation energies have been calculated as follows:

$$E_{imp}^s = E(\text{TiO}_{1-x}\text{N}_x) + \frac{x}{2}E(\text{O}_2) - E(\text{TiO}) - \frac{x}{2}E(\text{N}_2),$$

$$E_{imp}^v = E(\text{TiON}_x) - E(\text{TiO}) - \frac{x}{2}E(\text{N}_2),$$

where E^s and E^v are the energies of N implantation (indicated by the subindex *imp*) for substitutional and vacancy sites, respectively, $E(\text{TiO}_{1-x}\text{N}_x)$ and $E(\text{TiON}_x)$ are the total energies for the substitutionally and in-vacancy N-implanted systems, respectively, $E(\text{TiO})$ is the energy of the α -TiO system, and $E(\text{N}_2)$ and $E(\text{O}_2)$ are the energies of the isolated nitrogen and oxygen molecules. This definition implies implantation from $\text{N}_2(g)$. Since the N-N bond is very strong and very difficult to break, one could consider also the implantation process from atomic N. In fact, some times the experimental way to implant N is through ion bombardment. This second definition would involve the replacing of the terms $1/2E(\text{N}_2)$ by $E(\text{N})$ in the equations shown above, where $E(\text{N})$ is the energy of an isolated N atom. Although this choice might appear to be arbitrary, it allows us to make a direct comparison with previous work carried out on N implantation in TiO_2 .^{39,40} Indeed, a more complete treatment making use of chemical potentials is possible,^{71,72} however, in the present study, we are interested only in the relative energies and general tendencies and not in the exact values of the implantation energies.

In Table II we show the N-implantation energies for both definitions. The most stable site by far corresponds to the O-vacancy site, where the implanted N atom interacts with six Ti atoms in an octahedral environment. There are two energetically favorable contributions: electrostatic interaction of N^{3-} with six Ti cations and the covalent Ti-N interaction. This site is the optimal environment for the Ti-N interaction, i.e., the NaCl structure of TiN. The most unstable implantation site is by far in the Ti vacancy. In that site the implanted N atom interacts with six O atoms in an octahedral environment, and all contributions to the bond are unfavorable: electrostatic interaction of the N^{3-} with six O^{2-} anions and the covalent interactions Ti-N are prevented.

TABLE II. Substitutional and in-vacancy N-implantation energies in α -TiO from $N_2(g)$ and from atomic N. The range of analogous values for TiO_2 (Ref. 39) has been included for comparison (only the maximum and minimum values are shown).

Position	Implantation energies (eV)	
	From N_2	From N
Substitutional		
N-CV	2.25	-3.07
N-X	1.93	-3.39
N-Y	1.99	-3.33
TiO_2	5.53	0.20
	4.91	-0.41
Vacancy sites	From N_2	From N
O	-2.76	-8.08
Ti	4.96	-0.37
TiO_2 (O vacancy)	2.24	-3.08
	-0.57	-5.89

Finally, the implantation energies at substitutional places lie between the two situations mentioned above. There are three nonequivalent possibilities for the substitution, named in a previous work as N-X, N-Y, and N-CV.⁴⁸ Basically, N-X and N-Y are coordinated to five Ti atoms, they are pointing to an Ti vacancy, and they feel the electrostatic repulsion of the other five O^{2-} anions, with which they form the octahedral Ti-vacancy environment. N-CV is coordinated to four Ti atoms, pointing to two Ti vacancies (one above and the other below) and it feels the electrostatic repulsion of ten O^{2-} anions. The N-CV is more unstable than the others since the electrostatic repulsion in that site is multiplied by two with respect to the other two sites but the difference with the most stable substitutional site is only 0.32 eV.

It is interesting to note that the O-vacancy site is the only place in which the N implantation is thermodynamically favored from N_2 and that at the same time the implantation energy is high in that site (-2.76 eV). This indicates that the interaction of N- with the O-vacancy sites is so strong that it is able to break the N-N bond of the N_2 molecule. This is in contrast with what was observed in the O vacancies of TiO_2 .³⁹ In this oxide, among all the possible vacancies in the two outermost layers, only two vacancies in the second layer (subsurface) were found to be able to break the N-N bond of the N_2 molecule, with much smaller implantation energies than in the TiO case (-0.57 and -0.25 eV). In fact, high temperature is required experimentally for N implantation of TiO_2 even from NH_3 molecules.⁴⁰ The main difference is that in α -TiO there are a number of 3d electrons available for the incoming N atom, which needs three electrons for closing its shell (N^{3-}) but in TiO_2 the 3d band only contains two electrons per O vacancy. Another important difference is that in that site of the TiO system the incoming N atom is interacting favorably with six Ti cations (in the bulk) or five Ti cations (in the surface), with exactly the same symmetry than in the most stable nitride of titanium (TiN) but in TiO_2 the main vacancy is the bridging-O surface vacancy and in that

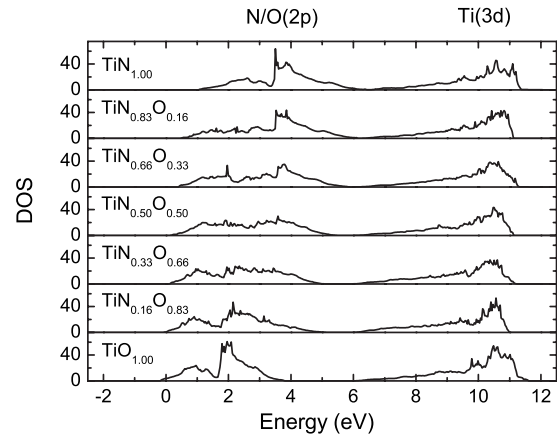


FIG. 5. Evolution of the DOS of the oxynitrides with the composition ($x:TiN_{1-x}O_x$) for the NaCl-type structure.

site the incoming N atom interacts with only two Ti atoms. Even if the incoming N atoms reach the substitutional sites of bulk TiO_2 , the higher Ti coordination attainable would then be three.

We have compared also the implantation energies of atomic N in α -TiO and rutile- TiO_2 . When the incoming N atoms go to the vacancy sites the range of values for the adsorption energy is -3.08 to -5.89 eV for rutile³⁹ while for TiO the adsorption energy in the vacancy is -8.08 eV. When we consider the substitutional sites the implantation energies lie within the range 0.20 to -0.41 eV for TiO_2 (Ref. 39) while the range for TiO is -3.07 to -3.39 eV. It is clear that the implantation of N is much easier in α -TiO than in TiO_2 . The reasons for that are the availability of 3d electrons to close the shell of the incoming N atoms and the better geometry of the implantation site (six-coordinated N atom with octahedral symmetry) which allows the optimal interaction between Ti and N.

E. Electronic structure

Finally, we studied the influence of the composition, geometrical structure, and initial N implantation on the electronic structure. First, we have to know the changes that the geometrical structure and composition ($TiN_{1-x}O_x$) induce in the electronic structure. In Fig. 5 and 6 we show the evolution of the density of states (DOS) with x for both structures (NaCl and α type). For both structures, the gap between the 2p(N/O) and 3d (Ti) bands increases as the concentration of O increases, and decreases as the concentration of N increases. In fact, in the α structure the 2p and 3d bands even collapse when all the O atoms have been replaced by N (see Fig. 6). In both structures we can modulate progressively the 2p-3d gap with the composition. The upper part of the 2p band corresponds mainly to N states and the bottom part corresponds to O states (see Fig. 7). For that reason, the 2p band moves progressively to higher energies when the concentration of N increases and to lower energies when the concentration of O increases, for both structures. The separation between the bands 2p and 3d as the concentration of O increases leads to a decrease in the 2p-3d mixing, which is

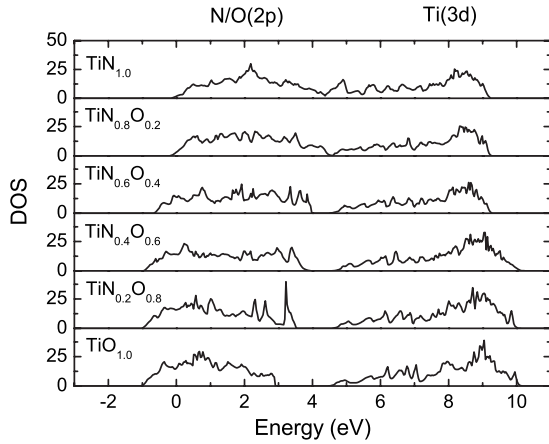


FIG. 6. Evolution of the DOS of the oxynitrides with the composition (x : $\text{TiN}_{1-x}\text{O}_x$) for the α -TiO structure.

related to the covalent contribution to the bond, and consequently the nature of the bond has a higher ionic contribution. This is in agreement with our previous study,⁴⁸ in which we showed that one of the most important factors for the stabilization of the defective α structure with respect to the compact NaCl-type structure was the strong ionic character of the solid. On the other hand, when the concentration of N increases, the approximation (and even collapse) of the 2p and 3d bands leads to an increase in the covalent character of the bond in the solid. Therefore, we can modulate the ionic-covalent character of the solid with the composition. This could be useful in catalytic applications and for controlling the surface reactivity.

Although the general trends are similar in both structures, there are some differences between them. In the NaCl-type structure the states of incoming atoms (O/N) never generate special states separated from the main 2p band but in the α -TiO structure the first substitutional incoming N atoms

generate little bands above the main 2p band [see Figs. 7(a), 7(b), 7(e), and 7(f)]. This is because all substitutional sites are always around a Ti vacancy and therefore there is a strong electrostatic repulsion between the N^{3-} species and the other O^{2-} anions around the octahedral Ti vacancy. Since the N states are always in the upper part of the 2p band, the electrostatic repulsion pushes some N states to higher energies and subsequently some states appear isolated from the main 2p band. In the NaCl-type structure the evolution of the states with the composition does not show isolated states since there are no vacancies and consequently there are no direct electrostatic repulsions between the N/O anions, which are surrounded by six Ti cations in a compact octahedral environment. The oxidation state of Ti changes progressively from Ti^{2+} (TiO) to Ti^{3+} (TiN) but the system remains a conductor since the Fermi level always falls in the 3d band. In TiO, each Ti atom has formally two 3d electrons and in TiN has one. Therefore, although the 2p-3d band gap can be controlled, the conductor character remains unchanged for the whole range of compositions for both structures.

The energetic considerations discussed above show that the incoming N atoms go first to the O vacancies. For that reason, we have also studied the effect of the presence of in-vacancies N atoms on the electronic structure [see Figs. 7(c) and 7(d)]. If we compare the electronic structure of substitutional N [Figs. 7(e) and 7(f)] and in-vacancy N [Figs. 7(c) and 7(d)], we find that the levels corresponding to in-vacancy N are always lower in energy. This can be seen clearly in the strong shift of the 2s band but we can also note that both the top and the main peak of the 2p band are shifted to lower energies. This means that N implantation in O vacancies stabilizes the system more than implantation in substitutional sites. This result is coherent with the thermodynamic analysis performed above (Sec. III D) about the first steps of N implantation (where we showed that the most stable implantation site is by far in the O vacancy) and can be explained in the same way.

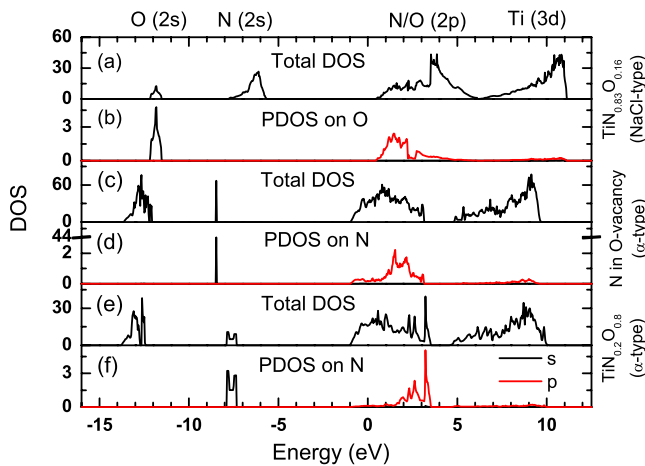


FIG. 7. (Color online) (a) Total and (b) projected on O atom DOS for the oxynitride with the NaCl-type structure of composition $\text{TiN}_{0.83}\text{O}_{0.16}$. (c) Total and (d) projected on N atom DOS for the oxynitride with α structure with N atoms implanted in the oxygen vacancies. (e) Total and (f) projected on N atom DOS for the oxynitride with α structure of composition $\text{TiN}_{0.2}\text{O}_{0.8}$ (substitutional N).

IV. CONCLUSIONS

We have shown, by means of DFT calculations, that there is no thermodynamic driving force inducing the segregation of titanium oxynitrides with composition $\text{TiN}_{1-x}\text{O}_x$. Therefore, there are theoretical reasons to state that these types of compounds are synthesizable. We have studied the evolution of the structures, as well as some of their properties. The cell volume increases as x increases for the NaCl-type structure while it decreases as x increases for the α -TiO structure. The limiting composition, in which the energetically preferred structure changes, is $x=0.55-0.6$, getting closer to 0.6 as the temperature increases. For compositions $x < 0.6$ the most stable arrangement of the system is in a NaCl-type structure while the α -TiO structure is more stable for compositions $x > 0.6$. The bulk moduli are always much larger for NaCl-type structures than for α -TiO, and they decrease as the amount of O increases, moving from 280 GPa for TiN- with NaCl-type structure to 197 GPa for α -TiO. The implantation of N in α -TiO has been found to be much easier than in TiO_2 because of two main reasons: (a) the availability of 3d elec-

trons to close the shell of incoming N atoms; and (b) the coordination of the incoming N atoms to five or six Ti atoms in an octahedral environment, which allows the optimal interaction between them. Initially the N atoms go to the O vacancies of the α -TiO (changing the composition to $\text{TiO}_{1.00}\text{N}_{0.25}$) and then the substitutional implantation process starts, leading to the NaCl-type structure when the N concentration is high enough. Finally, from an electronic point of view, we have shown that, although the solids with composition $\text{TiN}_{1-x}\text{O}_x$ are always conductors, it would be possible to modulate the covalent-ionic character of the bond in the

solid and the $2p$ - $3d$ band gap just by changing the composition. In the two structures (NaCl and α type), both the band gap and the ionic character increase as the concentration of O atoms increase.

ACKNOWLEDGMENTS

This work was funded by the Spanish Ministerio de Ciencia e Innovación, MICINN, projects MAT2008-04918 and Consolider-Ingenio CSD2008-00023.

*Corresponding author; sanz@us.es

- ¹L. E. Toth, *Transition Metal Carbides and Nitrides* (Academic, New York, 1971).
- ²J. E. Sundgren, *Thin Solid Films* **128**, 21 (1985).
- ³G. F. Hardy and J. K. Hulm, *Phys. Rev.* **93**, 1004 (1954).
- ⁴R. M. Fix, R. G. Gordon, and D. M. Hoffman, *Chem. Mater.* **2**, 235 (1990).
- ⁵J. B. Price, J. O. Borland, and S. Selbrede, *Thin Solid Films* **236**, 311 (1993).
- ⁶R. I. Hegde, R. W. Fiordalice, E. O. Travis, and P. J. Tobin, *J. Vac. Sci. Technol. B* **11**, 1287 (1993).
- ⁷M. Wittmer and H. Melchior, *Thin Solid Films* **93**, 397 (1982).
- ⁸C. Y. Ting and M. Wittmer, *Thin Solid Films* **96**, 327 (1982).
- ⁹I. Suni, M. Blomberg, and J. Saarihahti, *J. Vac. Sci. Technol. A* **3**, 2233 (1985).
- ¹⁰S. Kanamori, *Thin Solid Films* **136**, 195 (1986).
- ¹¹N. Kumar, K. Pourrezaei, B. Lee, and E. C. Douglas, *Thin Solid Films* **164**, 417 (1988).
- ¹²N. Kumar, J. T. McGinn, K. Pourrezaei, B. Lee, and E. C. Douglas, *J. Vac. Sci. Technol. A* **6**, 1602 (1988).
- ¹³H. Joswig, A. Kohlhase, and P. Hucher, *Thin Solid Films* **175**, 17 (1989).
- ¹⁴N. Yokoyama, K. Hinode, and Y. Homma, *J. Electrochem. Soc.* **136**, 882 (1989).
- ¹⁵R. Fix, R. G. Gordon, and D. M. Hoffman, *Chem. Mater.* **3**, 1138 (1991).
- ¹⁶U. Helmersson, S. Todorova, S. A. Barnett, J. E. Sundgren, L. C. Markett, and J. E. Greene, *J. Appl. Phys.* **62**, 481 (1987).
- ¹⁷S. Veprek, *J. Vac. Sci. Technol. A* **17**, 2401 (1999).
- ¹⁸S. Pisanec, L. C. Ciacchi, E. Vesselli, G. Comelli, O. Sbaizer, S. Meriani, and A. De Vita, *Acta Mater.* **52**, 1237 (2004).
- ¹⁹F. Vaz, P. Cerqueira, L. Rebouta, S. M. C. Nascimento, E. Alves, Ph. Goudeau, J. P. Rivière, K. Pischow, and J. de Rijk, *Thin Solid Films* **447-448**, 449 (2004).
- ²⁰S. Tsubota, M. Haruta, T. Kobayashi, A. Ueda, and Y. Ankara, in *Preparation of Catalysts V*, edited by G. Poncelet, P. A. Jacobs, P. Grange, and B. Delmon (Elsevier, Amsterdam, 1991), p. 695.
- ²¹M. K. Neylon, S. K. Bej, C. A. Bennett, and L. T. Thompson, *Appl. Catal., A* **232**, 13 (2002).
- ²²M. Grätzel, *Nature (London)* **414**, 338 (2001).
- ²³R. Asahi, T. Morikawa, T. Ohwaki, K. Aoki, and Y. Taga, *Science* **293**, 269 (2001).
- ²⁴T. L. Thompson and J. T. Yates, Jr., *Chem. Rev. (Washington, D.C.)* **106**, 4428 (2006).
- ²⁵T. Tachikawa, M. Fujitsuka, and T. Majima, *J. Phys. Chem. C* **111**, 5259 (2007).
- ²⁶J. Zhao, C. Chen, and W. Ma, *Top. Catal.* **35**, 269 (2005).
- ²⁷A. Fujishima and K. Honda, *Nature (London)* **238**, 37 (1972).
- ²⁸M. Valden, X. Lai, and D. W. Goodman, *Science* **281**, 1647 (1998).
- ²⁹M. S. Chen and D. W. Goodman, *Science* **306**, 252 (2004).
- ³⁰S. Lee, C. Fan, T. Wu, and S. L. Anderson, *J. Am. Chem. Soc.* **126**, 5682 (2004).
- ³¹I. N. Remediakis, N. Lopez, and J. K. Nørskov, *Angew. Chem., Int. Ed.* **44**, 1824 (2005).
- ³²N. C. Hernandez, J. F. Sanz, and J. A. Rodríguez, *J. Am. Chem. Soc.* **128**, 15600 (2006).
- ³³N. C. Saha and H. G. Tomkins, *J. Appl. Phys.* **72**, 3072 (1992).
- ³⁴J. Graciani, J. F. Sanz, T. Asaki, K. Nakamura, and J. A. Rodríguez, *J. Chem. Phys.* **126**, 244713 (2007).
- ³⁵K. Uetani, H. Kajiyama, A. Takagi, I. Tokomoto, Y. Koizumi, K. Nose, Y. Ihara, A. Kato, K. Onisawa, and T. Minemura, *Mater. Trans.* **42**, 403 (2001).
- ³⁶A. Glaser, S. Surnev, F. P. Netzer, N. Fateh, G. A. Fontalvo, and C. Mitterer, *Surf. Sci.* **601**, 1153 (2007).
- ³⁷L. C. Ciacchi, *Int. J. Mater. Res.* **2007**, 708.
- ³⁸M. Batzill, E. Morales, and U. Diebold, *Phys. Rev. Lett.* **96**, 026103 (2006).
- ³⁹J. Graciani, L. J. Álvarez, J. A. Rodríguez, and J. F. Sanz, *J. Phys. Chem. C* **112**, 2624 (2008).
- ⁴⁰J. Graciani, A. Nambu, J. Evans, J. A. Rodríguez, and J. F. Sanz, *J. Am. Chem. Soc.* **130**, 12056 (2008).
- ⁴¹C. Di Valentin, G. Pacchioni, and A. Selloni, *Phys. Rev. B* **70**, 085116 (2004).
- ⁴²C. Di Valentin, G. Pacchioni, A. Selloni, S. Livraghi, and E. Giamello, *J. Phys. Chem. B* **109**, 11414 (2005).
- ⁴³S. Livraghi, M. C. Paganini, E. Giamello, A. Selloni, C. Di Valentin, and G. Pacchioni, *J. Am. Chem. Soc.* **128**, 15666 (2006).
- ⁴⁴D. Watanabe, J. R. Castles, A. Jostsons, and A. S. Malin, *Nature (London)* **210**, 934 (1966).
- ⁴⁵D. Watanabe, J. R. Castles, A. Jostsons, and A. S. Malin, *Acta Crystallogr.* **23**, 307 (1967).
- ⁴⁶A. Taylor and N. J. Doyle, *High Temp. - High Press.* **1**, 679 (1969).
- ⁴⁷M. D. Banus, T. B. Reed, and A. J. Strauss, *Phys. Rev. B* **5**, 2775 (1972).
- ⁴⁸J. Graciani, A. Márquez, and J. F. Sanz, *Phys. Rev. B* **72**, 054117 (2005).

- ⁴⁹D.-H. Kang, D.-H. Ahn, M.-H. Kwon, H.-S. Kwon, K.-B. Kim, K.-S. Lee, and B.-K. Cheong, *Jpn. J. Appl. Phys., Part 1* **43**, 5243 (2004).
- ⁵⁰J.-M. Chappe, N. Martin, J. Lintymer, F. Sthal, G. Terwagne, and J. Takadoum, *Appl. Surf. Sci.* **253**, 5312 (2007).
- ⁵¹X. Yang, C. Li, B. Yang, W. Wang, and Y. Qian, *Chem. Phys. Lett.* **383**, 502 (2004).
- ⁵²Y. X. Leng, P. Yang, J. Y. Chen, H. Sun, J. Wang, G. J. Wang, N. Huang, X. B. Tian, and P. K. Chu, *Surf. Coat. Technol.* **138**, 296 (2001).
- ⁵³G. J. Wan, N. Huang, P. Yang, Y. X. Leng, H. Sun, J. Y. Chen, and J. Wang, *Thin Solid Films* **484**, 219 (2005).
- ⁵⁴R. Grau-Crespo, S. Hamad, C. R. A. Catlow, and N. H. de Leeuw, *J. Phys.: Condens. Matter* **19**, 256201 (2007).
- ⁵⁵G. Kresse and J. Joubert, *Phys. Rev. B* **59**, 1758 (1999).
- ⁵⁶J. Perdew, J. Chevary, S. Vosko, K. Jackson, M. Pederson, D. Singh, and C. Fiolhais, *Phys. Rev. B* **46**, 6671 (1992).
- ⁵⁷G. Kresse and J. Hafner, *Phys. Rev. B* **47**, 558 (1993).
- ⁵⁸G. Kresse and J. Furthmuller, *Comput. Mater. Sci.* **6**, 15 (1996); *Phys. Rev. B* **54**, 11169 (1996).
- ⁵⁹H. J. Monkhorst and J. D. Pack, *Phys. Rev. B* **13**, 5188 (1976).
- ⁶⁰J. Harris, *Phys. Rev. B* **31**, 1770 (1985); W. M. C. Foulkes and R. Haydock, *ibid.* **39**, 12520 (1989).
- ⁶¹R. Grau-Crespo, N. H. de Leeuw, and C. R. A. Catlow, *J. Mater. Chem.* **13**, 2848 (2003).
- ⁶²R. Grau-Crespo, N. H. de Leeuw, and C. R. A. Catlow, *Chem. Mater.* **16**, 1954 (2004).
- ⁶³N. Schönberg, *Acta Chem. Scand.* (1947-1973) **8**, 213 (1954).
- ⁶⁴V. A. Gubanov, A. L. Ivanovsky, and V. P. Zhukov, *Electronic Structure of Refractory Carbides and Nitrides* (Cambridge University Press, Cambridge, 1994).
- ⁶⁵Y. Syono, T. Goto, J. Nakai, Y. Nakagawa, and H. Iwasaki, *J. Phys. Soc. Jpn.* **37**, 442 (1974).
- ⁶⁶A. Taylor and N. J. Doyle, *J. Appl. Crystallogr.* **4**, 103 (1971).
- ⁶⁷*Handbook of Chemistry and Physics*, 87th ed., edited by D. R. Lide (Chemical Rubber, Cleveland, 2006), pp. 4–96, 5–16, and 12–24.
- ⁶⁸M. W. Chase, Jr., *NIST-JANAF Thermochemical Tables* Journal of Physical and Chemical Reference Data Monograph Vol. 9, 4th ed. (Springer, Berlin, 1998), pp. 1–1951.
- ⁶⁹M. Drygas, C. Czosnek, R. T. Paine, and J. F. Janik, *Chem. Mater.* **18**, 3122 (2006).
- ⁷⁰N. C. Hernández, J. Graciani, and J. F. Sanz, *Surf. Sci.* **541**, 217 (2003).
- ⁷¹N. D. M. Hine, K. Frensch, W. M. C. Foulkes, and M. W. Finnis, *Phys. Rev. B* **79**, 024112 (2009).
- ⁷²M. W. Finnis, A. Y. Lozovoi, and A. Alavi, *Annu. Rev. Mater. Res.* **35**, 167 (2005).